

## The effect of bismuth oxide addition on the electrical properties of zirconia–magnesia solid electrolytes

I. C. COSENTINO, R. MUCCILLO

*Instituto de Pesquisas Energéticas e Nucleares, Comissão Nacional de Energia Nuclear, CP 11049 Pinheiros, São Paulo, SP CEP 05422-970, Brazil*

Zirconia-based solid electrolytes are mostly used in oxygen sensors for the determination of oxygen activity in molten steels and in the regulation of combustion processes. They exhibit a relatively high oxygen-ion conductivity at temperatures suitable for the design of sensors. The sensor signal is an electromotive force (e.m.f.) generated between two faces of the electrolyte, one at a known oxygen potential and the other at the region to determine the oxygen activity. One of the requirements for the use of ceramic electrolytes as electrochemical devices is a density of >92% theoretical to avoid molecular oxygen ion diffusion, which could lead to erroneous determination of the sensor signal. Additives are used as sintering aids to decrease the sintering temperature and/or to inhibit grain growth in zirconia-based solid electrolytes.  $\text{Al}_2\text{O}_3$ ,  $\text{TiO}_2$  and  $\text{Bi}_2\text{O}_3$  have already been used mainly in yttria-stabilized zirconia [1, 2]. High relative densities and 5  $\mu\text{m}$  average grain size have been achieved at temperatures as low as 1150 °C in yttria-stabilized zirconia with bismuth oxide additions [3].

We report here a study of bismuth oxide additions in magnesia-partially stabilized zirconia (Mg-PSZ) solid electrolytes. Mg-PSZ has been used as solid electrolyte in disposable oxygen sensors for the determination of the oxygen content in molten steels [4]. The main purpose was to investigate the ability of bismuth oxide to act as sintering aid via reactive liquid-phase sintering in magnesia-stabilized zirconia, in the same way as it was done for yttria-stabilized zirconia [3]. The corrosive character of bismuth oxide poses no problem, due to the instantaneous measurement of the e.m.f. in the case of disposable sensors in the steel industry.

Zirconia–3 wt % magnesia coprecipitated powders and bismuth oxide powders were used. They were thoroughly mixed, pressed into pellets under 150 MPa and sintered at 1150 °C for 3 h (heating rate 100 °C h<sup>-1</sup>) in a platinum capsule which was placed in an alumina crucible filled with a powder mixture of magnesia-stabilized zirconia and 20% bismuth oxide, using an experimental configuration similar to that described by Winnubst and Burggraaf [3]. This procedure was followed to avoid bismuth oxide diffusion out of the sample. Some specimens were also quenched from 1550 °C in 1 h to favour cubic formation. Specimens for scanning electron microscopy (SEM) and electron microprobe (EMP) analyses had surfaces polished to 1  $\mu\text{m}$  followed by deposition of carbon. Specimens for a.c. impedance

measurements had Pt sputtered electrodes. The apparent densities of the sintered pellets were determined by the usual water-displacement method. X-ray diffraction analyses were performed with a Rigaku diffractometer. The ceramic structures of polished samples were investigated with a Cambridge Stereoscan S4 electron microscope. Two-probe d.c. resistivity measurements were carried out on an alumina sample chamber with Pt leads and a Pt/Pt–10% Rh thermocouple to monitor sample temperature, all inserted in a temperature-controlled tubular furnace. A 616 Keithley digital electrometer was used. Impedance spectroscopy measurements were carried out in the frequency range 5 Hz to 10 MHz with a Hewlett–Packard 4192A LF impedance analyser coupled to an HP 9000 controller, in the temperature range 300–650 °C.

Specimens with different bismuth oxide contents were prepared. The apparent densities and the d.c. resistivities in the electrolytic region were measured. Specimens with 5 wt % addition had higher density and lower electrical resistivity and were, consequently, chosen for the subsequent work. Table I gives the apparent densities of the sintered pellets (with and without 5 wt % bismuth oxide addition). With similar green densities, 89 and 99% theoretical densities were attained for specimens without and with  $\text{Bi}_2\text{O}_3$ , respectively. The 10% density enhancement was probably due to bismuth oxide pore filling via liquid-phase sintering.

X-ray diffractometry analyses of specimens sintered at 1150 °C showed only the characteristic monoclinic zirconia spectrum, as expected. Some specimens were further heated to 1550 °C followed by quenching to room temperature to look for conductivity enhancement due to cubic phase formation [5]. In this case X-ray diffractograms showed the typical cubic or tetragonal phase together with a remaining monoclinic phase. The monoclinic phase

TABLE I Densities of 3 wt % magnesia-partially stabilized zirconia without and with 5% bismuth oxide addition. Sintering was performed at 1150 °C for 3 h

Specimen	Green density (% theoretical)	Sintered density (% theoretical)
ZrO <sub>2</sub> :3 wt % MgO	52	89
ZrO <sub>2</sub> :3 wt % MgO + 5% Bi <sub>2</sub> O <sub>3</sub>	51	99

contents were determined according to Porter and Heuer [6] as approximately 70% for specimens with as well as without bismuth oxide. The remaining 30% are cubic and tetragonal phases. SEM analyses of fractured surfaces of these specimens were carried out. A micrograph is shown in Fig. 1.

Two different grain size distributions were observed: one with 8  $\mu\text{m}$  average grain size, probably due to the cubic phase, and the other with 2  $\mu\text{m}$  average grain size, due to monoclinic or tetragonal phases [7-9]. A detailed analysis of the micrographs of the fractured surface showed that 5% of the specimen volume had cubic phase. Therefore, the remaining 25% was tetragonal phase. In this case SEM analyses proved to be a powerful tool to distinguish cubic and tetragonal phases in zirconia, a difficult task if one relies solely on X-ray diffraction analysis [10]. EMP analyses were performed to evaluate the magnesium and bismuth distributions as well as the porosity of the samples: the magnesium distribution was found to be non-homogeneous and the average pore size was determined as 4  $\mu\text{m}$ . Quantitative analyses at five randomly chosen sites showed an average magnesium concentration of 0.2%. EMP analyses also showed that the addition of  $\text{Bi}_2\text{O}_3$  decreases specimen porosity, making clear that the additive takes intergranular position. Its distribution was also found to be inhomogeneous. Furthermore, SEM analyses also allowed the determination of the average magnesium agglomerate size as 2  $\mu\text{m}$ , in good agreement with the EMP values. EMP also showed that the grain boundaries of specimens with  $\text{Bi}_2\text{O}_3$  addition are Bi-enriched, as expected.

Fig. 2 shows Arrhenius plots of the d.c. resistivity of three samples:  $\text{ZrO}_2$ :3 wt % MgO,  $\text{ZrO}_2$ :3 wt % MgO with 5%  $\text{Bi}_2\text{O}_3$  addition sintered at 1150  $^\circ\text{C}$  for 3 h and the same but sintered at 1550  $^\circ\text{C}$  for 1 h.

The addition of bismuth oxide led to a decrease in the resistivity of the Mg-PSZ of approximately two orders of magnitude. Even samples heated to 1550  $^\circ\text{C}$ , well above the melting point of bismuth oxide (817  $^\circ\text{C}$ ), had lower resistivity, but higher than

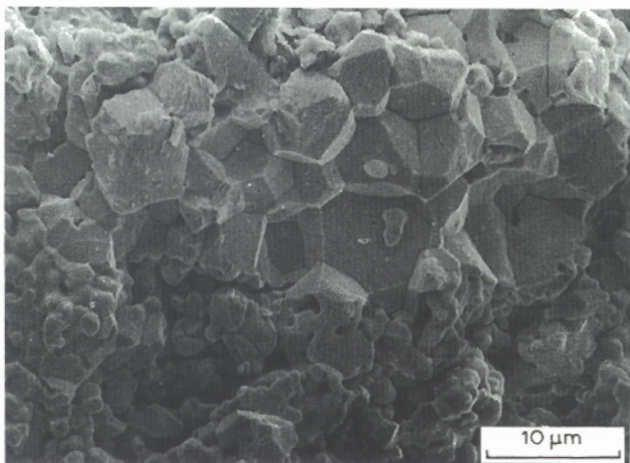


Figure 1 SEM micrograph of a fractured surface of zirconia: 3 wt % magnesia with 5 wt % bismuth oxide addition, sintered at 1150  $^\circ\text{C}$  for 3 h.

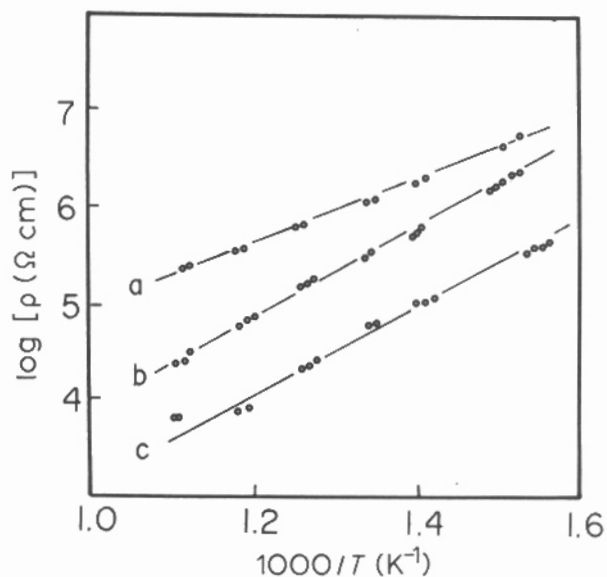


Figure 2 Arrhenius plots of the d.c. resistivity of: (a)  $\text{ZrO}_2$ :3 wt % MgO, (b)  $\text{ZrO}_2$ :3 wt % MgO +  $\text{Bi}_2\text{O}_3$  sintered at 1550  $^\circ\text{C}$  and (c)  $\text{ZrO}_2$ :3 wt % MgO +  $\text{Bi}_2\text{O}_3$  sintered at 1150  $^\circ\text{C}$ .

in samples sintered at 1150  $^\circ\text{C}$ , suggesting that the increase in conductivity due to cubic phase formation did not compensate the loss of bismuth oxide. That loss was actually seen in the alumina boats, which turned yellow after the high-temperature sintering. The presence of the remaining bismuth oxide in these samples was confirmed by energy-dispersive X-ray analysis. The activation energies were determined as 0.60 and 0.93 eV for specimens without and with bismuth oxide addition, respectively.

Fig. 3 shows complex impedance diagrams of zirconia-3 wt % magnesia and zirconia-3 wt % magnesia + 5 wt % bismuth oxide samples measured at 600  $^\circ\text{C}$ . Both samples were sintered at 1150  $^\circ\text{C}$  for 3 h.

The specimens with bismuth oxide as additive present two semicircles: one due to the resistivity of

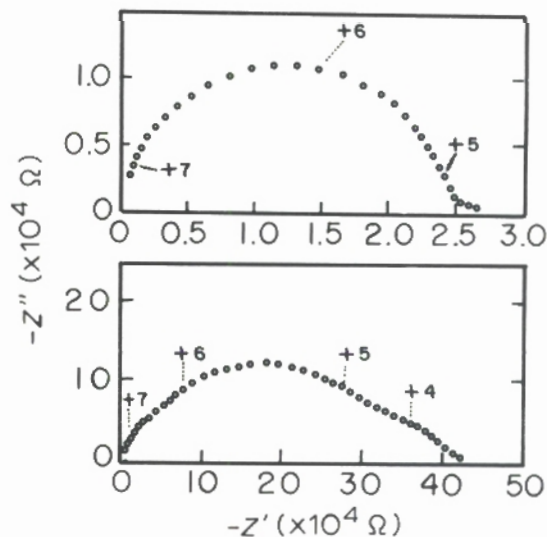


Figure 3 Impedance diagrams at 600  $^\circ\text{C}$  of sintered  $\text{ZrO}_2$ :3 wt % MgO with (top curve) and without (bottom) 5 wt %  $\text{Bi}_2\text{O}_3$  addition. Numbers indicate  $\log f$ .

the bulk and a smaller one due to the grain boundary resistivity. On the other hand, the impedance diagram of samples without bismuth oxide addition is not well resolved, with a relatively large grain boundary contribution. A preliminary analysis shows that the filling of intragrain regions by bismuth oxide reduces drastically the grain boundary resistivity. In other words, bismuth oxide acts as a conducting bridge for the oxygen ions from grain to grain. A detailed impedance spectroscopy analysis of the effect of the addition of bismuth oxide in zirconia-magnesia solid electrolytes is under way [11].

It may be concluded that the addition of bismuth oxide helps the densification as well as providing a higher ionic conductivity of zirconia-magnesia solid electrolytes for use in disposable sensors for the measurement of oxygen activity in molten steel.

### Acknowledgements

One of the authors (R.M.) thanks Professors M. Kleitz and L. Dessemond (Laboratoire d'Ionique et d'Electrochimie du Solide de Grenoble, France) for valuable help in the impedance spectroscopy work. We acknowledge Dr A. H. A. Bressiani for MEV analysis, Rejane A. Nogueira for EMP analyses and V. Ussui for preparing the coprecipitated powders. CNPq and RHAE scholarships are also acknowledged.

### References

1. K. C. RADFORD and R. J. BRATTON, *J. Mater. Sci.* **14** (1979) 59.
2. K. KEIZER, A. J. BURGGRAAF and G. DE WITH, *ibid.* **17** (1982) 1095.
3. A. J. A. WINNUBST and A. J. BURGGRAAF, *Mater. Res. Bull.* **19** (1984) 613.
4. K. P. JAGANNATHAN, S. K. TIKU, H. S. RAY, A. GHOSH and E. C. SUBBARAO, in "Solid electrolytes and their applications", edited by E. C. Subbarao (Plenum Press, New York, 1980) p. 201.
5. E. P. BUTLER, R. K. SLOTWINSKI, N. BONANOS, J. DRENNAN and B. C. H. STEELE, in "Advances in ceramics", Vol. 12: "Science and technology of zirconia II", edited by N. Claussen, M. Rühle and A. H. Heuer (American Ceramics Society, Westerville, Ohio, 1984) p. 572.
6. D. L. PORTER and H. HEUER, *J. Amer. Ceram. Soc.* **62** (1979) 298.
7. M. RÜHLE, N. CLAUSSEN and A. H. HEUER, in "Advances in ceramics", Vol. 12: "Science and technology of zirconia II", edited by N. Claussen, M. Rühle and A. H. Heuer (American Ceramics Society, Westerville, Ohio, 1984) p. 352.
8. R. CHAIM and A. H. HEUER, *J. Amer. Ceram. Soc.* **83** (1986) 243.
9. F. C. WU and S. C. YU, *Mater. Res. Bull.* **23** (1988) 1773.
10. R. SRINIVASAN, R. J. DE ANGELIS, G. ICE and B. H. DAVIS, *J. Mater. Res.* **6** (1991) 1287.
11. R. MUCCILLO, unpublished results.

Received 29 September 1992  
and accepted 1 February 1993